

# KALE: When Energy-Based Learning Meets Adversarial Training

Michael Arbel<sup>1</sup> Liang Zhou<sup>1</sup> Arthur Gretton<sup>1</sup>

## Abstract

Legendre duality provides a variational lower-bound for the Kullback-Leibler divergence (KL) which can be estimated using samples, without explicit knowledge of the density ratio. We use this estimator, the *KL Approximate Lower-bound Estimate* (KALE), in a contrastive setting for learning energy-based models, and show that it provides a maximum likelihood estimate (MLE). We then extend this procedure to adversarial training, where the discriminator represents the energy and the generator is the base measure of the energy-based model. Unlike in standard generative adversarial networks (GANs), the learned model makes use of both generator and discriminator to generate samples. This is achieved using Hamiltonian Monte Carlo in the latent space of the generator, using information from the discriminator, to find regions in that space that produce better quality samples. We also show that, unlike the KL, KALE enjoys smoothness properties that make it suitable for adversarial training, and provide convergence rates for KALE when the negative log density ratio belongs to the variational family. Finally, we demonstrate the effectiveness of this approach on simple datasets.

## 1. Introduction

We consider the problem of learning energy-based models (EBMs), which have a long history in physics, statistics and machine learning (LeCun et al., 2006). EBMs can be described as a family of unnormalized probability distributions with a common *base* distribution  $\mathbb{Q}$  and an *energy* function  $f$ . Each distribution is normalized by the *partition function*  $Z(f)$ . The base  $\mathbb{Q}$  represents a state of maximum entropy for the system, while the energy  $f$  encodes information about which configurations are most likely. Given a class of possible energy functions, the learning task consists of find-

<sup>1</sup>Gatsby Computational Neuroscience Unit, University College London. Correspondence to: Michael Arbel <michael.n.arbel@gmail.com>.

*Work in progress.*

ing an optimal function that best describes a given system or target distribution  $\mathbb{P}$ . This can be achieved using maximum likelihood estimation (MLE); however, the intractability of the normalizing partition function makes this learning task challenging. Thus, various methods have been proposed to circumvent this.

*Contrastive Divergence* (Hinton, 2002) approximates the gradient of the log-likelihood by sampling from the energy model with Markov Chain Monte Carlo. More recently, (Du & Mordatch, 2019) extend the idea using more sophisticated sampling strategies that lead to high quality estimators. *Score Matching* (Hyvärinen, 2005) calculates an alternative objective (the *score*) to the log-likelihood. The score has the advantage of being independent of the partition function, and under mild smoothness conditions, is shown to be a valid alternative to the maximum likelihood. It was more recently used in the context of kernel methods and non-parametric energy functions to provide estimators of the energy that are provably consistent (Sriperumbudur et al., 2017; Sutherland et al., 2018; Arbel & Gretton, 2018; Wenliang et al., 2019). In *Noise-Contrastive Estimation*, a classifier is trained to distinguish between samples from a fixed proposal distribution and the target distribution (Gutmann & Hyvärinen, 2012). This provides an estimate for the density ratio between the optimal energy model and the proposal distribution. In more recent work, (Dai et al., 2019a;b) exploit a dual formulation of the logarithm of the partition function as a supremum of some functional objective over the set of all probability distributions. This allows them to formulate the MLE problem as a minimax problem over functional spaces.

In the present work, we present a new approach to fitting energy based models using a variational lower bound on the Kullback-Leibler (KL) divergence between the base distribution  $\mathbb{Q}$  and the target distribution  $\mathbb{P}$ . We call this bound the **KL Approximate Lower-bound Estimate (KALE)**. The bound exploits *Fenchel duality*, as in (Nguyen et al., 2010; Nowozin et al., 2016; Dai et al., 2019a;b), and can be estimated using samples from both the base and the target distributions by solving an optimization problem. The optimization can be performed using stochastic gradient descent and automatic differentiation, allowing for scalability and modularity. We show that estimating KALE provides an MLE solution when the variational family is chosen to be

the class of energies augmented with constants. Hence, the MLE can be approximated using a simple algorithm which doesn't require directly estimating the partition function, nor does it require introducing additional surrogate models, as done in variational inference (Kingma & Welling, 2014; Rezende et al., 2014). When the *negative log density ratio* between the target  $\mathbb{P}$  and the base  $\mathbb{Q}$  is contained in the variational family,  $\text{KALE}(\mathbb{P}||\mathbb{Q})$  is in fact equal to the  $\text{KL}(\mathbb{P}||\mathbb{Q})$ . We provide convergence rates for the estimator of KALE when the variational family is a Hilbert space. While (Nguyen et al., 2010) provide rates for a similar estimator, these require the strong assumption that the density ratio is bounded above and below, which we do not require.

When the base  $\mathbb{Q}$  can also be learned as an implicit model supported on a lower-dimensional manifold, using  $\text{KL}(\mathbb{P}||\mathbb{Q})$  as a loss leads to instability (Arjovsky et al., 2017). While this suggests that KALE would inherit the same instability, we show that it actually depends on the choice of the energy function and base distributions. More precisely, following recent work (Chu et al., 2020; Sanjabi et al., 2018), we provide smoothness conditions which ensure that KALE is a valid optimization objective for the parameters of the base distribution. Such conditions can be ensured in practice using various regularization techniques (Miyato et al., 2018; Gulrajani et al., 2017).

This offers the opportunity to utilize KALE in an adversarial setting, with a training procedure that alternates between estimating the energy function and the base distribution, by analogy with  $f$ -GAN training (Goodfellow et al., 2014; Nowozin et al., 2016). Our approach is different, however, since it combines both the base distribution *and* the energy into a single model to produce samples. We use a Hamiltonian Monte Carlo sampler on the latent noise, with samples then mapped to the observation space using the learned base function. We show that the proposed sampling procedure provably converges towards the model distribution by leveraging recent work from (Eberle et al., 2017). Intuitively, the sampling procedure allows the model to use information learned by the energy function to find regions in the latent space that produce better quality samples. While there has been a recent interest in using the discriminator/energy to improve the quality of the generator/base (Azadi et al., 2019; Grover et al., 2019; Turner et al., 2019; Tanaka, 2019) (Section 5), our approach emerges naturally from the energy model we consider.

In Section 2 we provide some background on energy-based models, implicit generative models, and Fenchel duality for the KL. This sets the ground for introducing the KALE in Section 3, where we also explain the connection between KALE and MLE. We also derive a method for sampling from the learned model when the base is defined through an implicit generative model. In Section 4 we prove useful

properties of KALE that allow it to be used in training implicit models, such as smoothness and convergence rates. Section 5 discusses related work, and the experiments in Section 6 demonstrate that samples from EBMs are qualitatively better than those obtained solely from the generator.

## 2. Background

### 2.1. Energy-Based Models

An *energy-based model* (EBM) is defined by a set  $\mathcal{E}$  of real valued functions called *energies* along with a fixed distribution  $\mathbb{Q}$  called the *base*, all of which are defined on an input space  $\mathcal{X} \subset \mathbb{R}^d$ . The EBM is then given by the class of Boltzmann distributions of the form

$$d\mathbb{P}_{f,\mathbb{Q}}(x) = \frac{\exp(-f(x))}{Z(f)} d\mathbb{Q}(x), \quad (1)$$

where  $Z(f) = \int \exp(-f) d\mathbb{Q}$  is the *partition function* for a given  $f \in \mathcal{E}$ . In this work,  $\mathcal{E}$  can be either parametric (such as neural networks) or non-parametric. Examples of non-parametric spaces are Reproducing Kernel Hilbert Spaces (RKHS) as considered in (Canu & Smola, 2006; Fukumizu, 2009; Sriperumbudur et al., 2017). When  $\mathcal{E}$  is parametric, the function  $f \in \mathcal{E}$  is parametrized by some finite-dimensional vector  $\psi$  in a parameter space  $\Psi$  and will often be denoted  $f_\psi$ . The aim of energy-based learning is to find an optimal energy function  $f^*$  for which the corresponding Boltzmann distribution  $\mathbb{P}_{f^*,\mathbb{Q}}$  best approximates some given target distribution  $\mathbb{P}$ . When  $\mathbb{Q}$  admits a density  $q$  w.r.t. to the Lebesgue measure  $dx$ , a common approach is to maximize the expected log-likelihood of the model under  $\mathbb{P}$

$$\mathcal{L}(f, \mathbb{P}) = \int (\log(q) - f) d\mathbb{P} - \log(Z(f)). \quad (2)$$

In the parametric case, (2) can be solved using gradient descent under suitable smoothness assumptions provided that  $Z(f)$  has a closed form expression. However, for more complex energy models, the partition function is often intractable, making direct estimation of (2) challenging.

### 2.2. Implicit Generative Models

As considered in (Goodfellow et al., 2014), an *implicit generative model* (IGM) is a family of probability distributions  $\mathbb{Q}_\theta$  parametrized by some vector  $\theta \in \Theta$  which aims to approximate a target distribution  $\mathbb{P}$ . It is defined through a *generator* function  $g_\theta : \mathcal{Z} \mapsto \mathcal{X}$  that maps latent samples  $z$  from a fixed latent distribution  $\eta$  to the input space  $\mathcal{X}$ . When the latent space  $\mathcal{Z}$  has a smaller dimension than the input space  $\mathcal{X}$ , the IGM will typically be supported on a lower dimensional manifold<sup>1</sup> of  $\mathcal{X}$  and will thus not possess

<sup>1</sup>Here, the notion of manifold is considered in a loose sense and does not necessarily assume a smooth structure.

a Lebesgue density on  $\mathcal{X}$  (Bottou et al., 2017). IGMs are often trained by minimizing a cost functional that depends on samples from both the target  $\mathbb{P}$  and the generator  $\mathbb{Q}_\theta$ . The loss can be expressed as a supremum of some variational objective over a function class  $\mathcal{H}$ :

$$\mathcal{D}(\mathbb{P}, \mathbb{Q}_\theta) := \sup_{h \in \mathcal{H}} - \int h \, d\mathbb{P} - \int c \circ h \, d\mathbb{Q}_\theta, \quad (3)$$

where  $c : \mathbb{R} \rightarrow \mathbb{R}$  is some fixed concave real valued function. When  $c(x) = -x$ , the discrepancy  $\mathcal{D}(\mathbb{P}, \mathbb{Q}_\theta)$  belongs to the class of *Integral Probability Metrics* (IPM) (Arjovsky et al., 2017; Li et al., 2017; Bińkowski et al., 2018), while other choices lead to general  $f$ -divergences (Nowozin et al., 2016). In practice, the IGM is learned by alternating optimization over the *generator*  $g_\theta$  and the *discriminator*  $h \in \mathcal{H}$  defined in (3) in a procedure called *adversarial training* (Goodfellow et al., 2014). In the next section, we consider a particular choice for  $c$  which is closely related to the KL divergence.

### 2.3. Fenchel Duality for the KL divergence

A distribution  $\mathbb{P}$  is said to admit a density w.r.t.  $\mathbb{Q}$  if there exists a real-valued measurable function  $r_0$  that is integrable w.r.t.  $\mathbb{Q}$  and satisfies  $d\mathbb{P} = r_0 d\mathbb{Q}$ . Such a density is also called the *Radon-Nikodym derivative* of  $\mathbb{P}$  w.r.t.  $\mathbb{Q}$ . In this case, we have:

$$\text{KL}(\mathbb{P}||\mathbb{Q}) = \int r_0 \log(r_0) d\mathbb{Q}. \quad (4)$$

(Nguyen et al., 2010; Nowozin et al., 2016) derived a variational formulation for the KL using Fenchel duality. By the duality theorem (Rockafellar, 1970), the convex and lower semi-continuous function  $\zeta : u \mapsto u \log(u)$  that appears in (4) can be expressed as the supremum of a concave function:

$$\zeta(u) = \sup_v uv - \zeta^*(v). \quad (5)$$

The function  $\zeta^*$  is called the *Fenchel dual* and is defined as  $\zeta^*(v) = \sup_u uv - \zeta(u)$ . By convention, the value of the objective is set to  $-\infty$  whenever  $u$  is outside of the domain of definition of  $\zeta^*$ . When  $\zeta(u) = u \log(u)$ , the Fenchel dual  $\zeta^*(v)$  admits a closed form expression of the form  $\zeta^*(v) = \exp(v - 1)$ . Using the expression of  $\zeta$  in terms of its Fenchel dual  $\zeta^*$ , it is possible to express  $\text{KL}(\mathbb{P}||\mathbb{Q})$  as the supremum of the variational objective (6) over all measurable functions  $h$ .

$$\mathcal{F}(h) := - \int h \, d\mathbb{P} - \int \exp(-h) \, d\mathbb{Q} + 1. \quad (6)$$

Hence, the KL divergence is actually a particular case of (3) with the functional space  $\mathcal{H}$  being the set of all measurable functions and its supremum achieved exactly for  $h = -\log(r_0)$ . In (Nguyen et al., 2010), the variational

formulation was provided for the reverse KL using a different choice for  $\zeta$ :  $(\zeta(u) = -\log(u))$ . We refer to (Nowozin et al., 2016) for general  $f$ -divergences. In the next section, we can consider the effect of choosing a different set of functions  $\mathcal{H}$ , which generally leads to a lower bound on the KL.

### 3. KL Approximate Lower-bound Estimate

The *KL Approximate Lower-bound Estimate* (KALE) is obtained by restricting the variational objective (6) to a smaller class of functions  $\mathcal{H}$ :

$$\text{KALE}(\mathbb{P}||\mathbb{Q}) = \sup_{h \in \mathcal{H}} \mathcal{F}(h) \quad (7)$$

In general,  $\text{KL}(\mathbb{P}||\mathbb{Q}) \geq \text{KALE}(\mathbb{P}||\mathbb{Q})$ . The bound is tight whenever the negative log-density  $h_0 = -\log r_0$  belongs to  $\mathcal{H}$ ; however, we do not require  $r_0$  to be well-defined. Equation (7) has the advantage that it can be estimated using samples from  $\mathbb{P}$  and  $\mathbb{Q}$ . Given i.i.d. samples  $(X_1, \dots, X_N)$  and  $(Y_1, \dots, Y_N)$  from  $\mathbb{P}$  and  $\mathbb{Q}$ , we denote by  $\hat{\mathbb{P}}$  and  $\hat{\mathbb{Q}}$  the corresponding empirical distributions. A simple approach to estimate  $\text{KALE}(\mathbb{P}||\mathbb{Q})$  is to use an  $M$ -estimator. This is achieved by optimizing the penalized objective

$$\hat{h} := \arg \max_{h \in \mathcal{H}} \hat{\mathcal{F}}(h) - \frac{\lambda}{2} I^2(h), \quad (8)$$

where  $\hat{\mathcal{F}}$  is an empirical version of  $\mathcal{F}$  and  $I^2(h)$  is a penalty term that prevents overfitting due to finite samples. The penalty  $I^2(h)$  acts as a regularizer favoring smoother solutions while the parameter  $\lambda$  determines the strength of the smoothing and is chosen to decrease as the sample size  $N$  increases. A typical choice for the penalty  $I(h)$  is  $\|h\|$  when  $\mathcal{H}$  is a Hilbert space, as discussed in more details in Section 4.2. The  $M$ -estimator of  $\text{KALE}(\mathbb{P}||\mathbb{Q})$  is obtained simply by plugging in  $\hat{h}$  into the empirical objective  $\hat{\mathcal{F}}(h)$ :

$$\widehat{\text{KALE}}(\mathbb{P}||\mathbb{Q}) := \hat{\mathcal{F}}(\hat{h}). \quad (9)$$

We defer the consistency analysis of (9) to Section 4.2 where we provide convergence rates in a setting that was not covered by the framework of (Nguyen et al., 2010). First, we show how KALE allows us to compute the MLE of a suitable EBM.

#### 3.1. Learning Energy-Based Models with KALE

As discussed in Section 2.1, EBMs can be learned by maximizing the log-likelihood in (2). However, the partition function  $Z(f)$  is often intractable, which makes the estimation challenging. Instead, we will approximate the KALE using samples from both the target and the base, which will lead to the MLE solution. Here, we are interested in the general case where the base  $\mathbb{Q}$  is not required to admit a density

$q$ . This can happen if  $\mathbb{Q}$  is obtained from an implicit model as discussed in Section 2.2. In this case, the expression of the likelihood in (2) cannot be used, so we instead introduce a generalized notion of likelihood that is compatible with more general bases  $\mathbb{Q}$ , including those of implicit models.

**Definition 1** (Generalized Likelihood). *Assume that the EBM in (1) admits a density  $(r_f)_{f \in \mathcal{E}}$  w.r.t. to some fixed measure  $\mu$ . The expected  $\mu$ -log-likelihood of the model  $\mathbb{P}_{f, \mathbb{Q}}$  under a target distribution  $\mathbb{P}$  is then defined as:*

$$\mathcal{L}_\mu(f, \mathbb{P}) := \int \log(r_f) d\mathbb{P}. \quad (10)$$

Definition 1 subsumes the standard likelihood considered in (2). Indeed, when  $\mu$  is chosen to be the Lebesgue measure and whenever  $\mathbb{Q}$  admits a density  $q$  w.r.t. to  $\mu$ , it is easy to see that (2) and (10) are in fact the same. On the other hand, when  $\mu$  is chosen to be equal to the base  $\mathbb{Q}$ , one obtains the expected  $\mathbb{Q}$ -log-likelihood. This is well-defined even when  $\mathbb{Q}$  doesn't admit a density, as it only depends on the energy function  $f$  and the partition function  $Z(f)$ :

$$\mathcal{L}_{\mathbb{Q}}(f, \mathbb{P}) := - \int f d\mathbb{P} - \log(Z(f)). \quad (11)$$

In fact, we can show that (11) is closely related to the variational objective in (6):

**Proposition 1.** *The following identity holds:*

$$\mathcal{L}_{\mathbb{Q}}(f, \mathbb{P}) = \sup_{c \in \mathbb{R}} \mathcal{F}(f + c). \quad (12)$$

Proposition 1 is a direct consequence of the concavity of the logarithm function. More precisely, for all  $c \in \mathbb{R}$  one has

$$-c - \log(Z(f + c)) \geq -c - Z(f + c) + 1.$$

The equality holds when the right hand side is maximized w.r.t.  $c$ , the optimal value for  $c$  being  $c^* = \log(Z(f))$ . This suggests a choice for the variational space  $\mathcal{H}$  in (7) of the simple form

$$\mathcal{H} = \mathcal{E} + \mathbb{R}.$$

The constant term accounts for the total mass of the EBM when estimating KALE, but it does not change the model itself; in other words:  $\mathbb{P}_{f+c, \mathbb{Q}} = \mathbb{P}_{f, \mathbb{Q}}$  for any  $c \in \mathbb{R}$ . The *Noise-Contrastive Estimation* framework of (Gutmann & Hyvärinen, 2012) also introduced an additional variable to learn the partition function by using a classification objective between a target distribution and a known noise distribution for density ratio estimation. Here, we instead propose to maximize the variational objective (6) on  $\mathcal{H}$ , which automatically increases the likelihood thanks to (12). We discuss this connection in more detail in Section 5.

Unlike the widely known *Evidence Lower Bound* (ELBO) (Jordan et al., 1999) in Bayesian optimization, (12) doesn't introduce a surrogate model. In fact, a stronger result holds relating the MLE solution to KALE:

### Algorithm 1 KALE-energy

---

```

1: Input  $N, \lambda, n_{\mathcal{E}}, \gamma_{\mathcal{E}}, h_0, \mathbb{P}, \mathbb{Q}$ ,
2: Output  $h_{n_{\mathcal{E}}}$ 
3: Set  $(\psi, c) \leftarrow (\psi_0, c_0)$  where  $h_0 = f_{\psi_0} + c_0$ 
4: for  $k = 0, \dots, n_{\mathcal{E}} - 1$  do
5:    $X_i \sim \mathbb{P}$  and  $Y_i \sim \mathbb{Q}$  for  $1 \leq i \leq N$ 
6:   Compute gradient of  $\widehat{\mathcal{F}}(h_k) - \frac{\lambda}{2} I(h_k)^2$  w.r.t.  $(\psi, c)$ :
       $(\Delta\psi, \Delta c) \leftarrow \nabla_{(\psi, c)} \widehat{\mathcal{F}}(h_k) - \lambda I(h_k) \nabla_{(\psi, c)} I(h_k)$ 
7:   Update model  $h_{k+1}$ :
       $(\psi, c) \leftarrow (\psi, c) + \gamma_{\mathcal{E}}(\Delta\psi, \Delta c)$ 
       $h_{k+1} \leftarrow f_{\psi} + c$ 
8: end for

```

---

**Proposition 2.** *When  $\mathcal{H}$  is of the form  $\mathcal{H} = \mathcal{E} + \mathbb{R}$ , the following holds:*

$$\sup_{f \in \mathcal{E}} \mathcal{L}_{\mathbb{Q}}(f, \mathbb{P}) = \sup_{h \in \mathcal{H}} \mathcal{F}(h) = \text{KALE}(\mathbb{P} \parallel \mathbb{Q}). \quad (13)$$

Proposition 2 implies that maximizing the variational objective in (6) always leads to an MLE solution of the energy model, therefore providing a practical way to learn EBMs without directly dealing with the intractable partition function. Moreover, unlike the ELBO, the optimal solution of the variational objective  $\mathcal{F}$  is always tight. In the parametric setting, it is therefore possible to find the MLE solution by solving the regularized problem (8) in a stochastic setting as described by Algorithm 1.

When  $\mathbb{P}$  has more mass in low density regions of  $\mathbb{Q}$ , the optimal energy  $f^*$  corresponding to the MLE solution needs to compensate for this mismatch by having a singular-looking landscape. To address this problem, we consider learning the base distribution  $\mathbb{Q}$  as well by minimizing  $\text{KALE}(\mathbb{P} \parallel \mathbb{Q})$ . The ability to easily produce samples from  $\mathbb{Q}$  is retained by choosing an IGM as defined in Section 2.2. The training procedure simply alternates between learning an EBM with a fixed base given by a generator  $\mathbb{Q}_\theta$  and optimizing that base in order to decrease  $\text{KALE}(\mathbb{P} \parallel \mathbb{Q}_\theta)$ . While this procedure is in practice similar to adversarial training (Goodfellow et al., 2014), the resulting model is an EBM with an optimized base distribution of the form  $d\mathbb{P}^* \propto \exp(-f^*) d\mathbb{Q}_{g_{\theta^*}}$ . This is summarized in Algorithm 3 of Appendix C. As we discuss in Section 4.1, KALE satisfies desirable smoothness properties w.r.t. the parameters of the base which makes it a valid cost function, therefore justifying the adversarial training procedure. This stands in contrast to the KL, which can be undefined and non-smooth w.r.t. the parameters of the base (Arjovsky et al., 2017).

### 3.2. Sampling from Energy models

As discussed in Section 3.1, the output of Algorithm 3 is an EBM with an optimized base distribution  $\mathbb{Q}_{\theta^*}$ . Therefore,

sampling from the base distribution only, as usually done in the context of GANs, would discard information learned by the EBM. On the other hand, since the model doesn't generally admit a density w.r.t. the Lebesgue measure, it is not possible to directly use standard MCMC methods on the sample space. Instead, we propose to perform a variant of Hamiltonian Monte Carlo in the latent space  $\mathcal{Z}$  of the base generator. More precisely, instead of sampling the latent noise from the *prior distribution*  $d\eta$ , we propose to sample from the un-normalized *posterior distribution* given by  $d\eta_{z|\mathbb{P}}(z) \propto d\eta(z) \exp(-f^*(g_{\theta^*}(z)))$  using Langevin Monte Carlo and then apply the mapping  $g_{\theta^*}$  to obtain samples from the MLE model. We later show in Proposition 3 that such a procedure indeed produces samples from the EBM.

For clarity, we first consider the continuous time version of the sampler. We assume that the latent distribution  $\eta$  is a standard Gaussian over the latent space  $\mathcal{Z} := \mathbb{R}^r$  and let  $U(z) = \frac{1}{2}\|z\|^2 + f^* \circ g_{\theta^*}(z)$  be the energy function of the latent posterior  $d\eta_{z|\mathbb{P}}(z)$ . The Langevin dynamics with friction in an augmented space  $\mathbb{R}^{2r}$  are given by:

$$\begin{aligned} dz_t &= v_t dt \\ dv_t &= -(\kappa v_t + \nabla U(z_t)) + \sqrt{2\kappa} dw_t \end{aligned} \quad (14)$$

where  $v_t$  is a velocity vector,  $\kappa > 0$  is a friction parameter and  $w_t$  is Brownian motion. This choice of dynamics comes with convergence guarantees. Indeed, Proposition 3 shows that the process  $x_t = g_{\theta^*}(z_t)$  converges to the desired MLE distribution  $\mathbb{P}_{g_{\theta^*}} \exp^{-f^*}$  at a linear rate. This is a consequence of (Eberle et al., 2017) (Corollary 2.6) as shown in Appendix A.1 and simply requires the generator and energy function be smooth.

**Proposition 3.** *Under Assumptions (II) and (IV) in Appendix A.2, the distribution  $\mathbb{P}_t$  of the process  $x_t$  converges towards the MLE distribution  $\mathbb{P}_{f^*, \mathbb{Q}_{\theta^*}} := \mathbb{P}_{g_{\theta^*}} \exp(-h^*)$  at a linear rate in the Wasserstein sense, i.e.:*

$$W_2^2(\mathbb{P}_t, \mathbb{P}_{f^*, \mathbb{Q}_{\theta^*}}) \leq C e^{-ct} \quad (15)$$

where  $c$  and  $C$  are positive constants.

As the latent space  $\mathcal{Z}$  typically has a dimension that is orders of magnitude smaller than the input space dimension, the dynamics defined in (14) will have better mixing properties than procedures which directly sample from the input space. The resulting process  $(\mathbb{P}_t)_t$  on the input space  $\mathcal{X}$  can be informally regarded as a diffusion process on a general metric-measure space in the sense of (Sturm, 1998). Exploring such connections more formally would be an interesting research direction. In practice, to obtain samples from  $\mathbb{P}_t$ , we use a discretization similar to (Sachs et al., 2017) based on Leapfrog integration as shown in Algorithm 2.

## Algorithm 2 Langevin Monte Carlo

---

```

1: Input  $(Z_0, V_0), \gamma, \kappa, g_\theta$ 
2: Ouput  $X_T$ 
3: for  $t = 0, \dots, T$  do
4:    $Z_{t+\frac{1}{2}} \leftarrow Z_t + \frac{\gamma}{2} V_t$ 
5:    $V_{t+\frac{1}{2}} \leftarrow V_t - \frac{\gamma}{2} \nabla U(Z_{t+\frac{1}{2}})$ 
6:    $\tilde{V}_{t+1} \leftarrow \exp(-\kappa\gamma) V_{t+\frac{1}{2}} + \sqrt{1 - \exp(-2\kappa\gamma)} \xi_{t+1}$ 
7:    $V_{t+1} \leftarrow \tilde{V}_{t+1} - \frac{\gamma}{2} \nabla U(Z_{t+\frac{1}{2}})$ 
8:    $Z_{t+1} \leftarrow Z_{t+\frac{1}{2}} + \frac{\gamma}{2} V_{t+1}$ 
9: end for
10:  $X_T \leftarrow g_\theta(Z_T)$ 

```

---

## 4. Properties of KALE

### 4.1. Smoothness properties

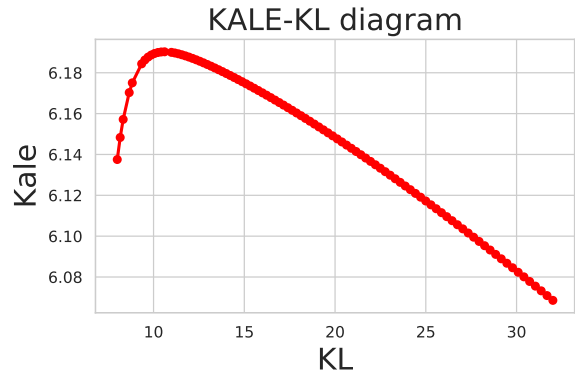


Figure 1: KALE vs KL between two varying probability distributions. The example consists of two Gaussians of standard deviation 0.5 that are reparametrized using a logit-like non-linearity. One of the Gaussians is centered at the origin, while the center of the second one is moving further away from the origin. At the same time, the non-linearity is chosen to be flatter at the origin. To compute KALE,  $\mathcal{H}$  is chosen to be a RKHS with a gaussian kernel of bandwidth 1. The squared RKHS norm of the energy is used as a penalty, with a strength of  $10^{-4}$ . KALE is estimated using 1000 samples using the CVX solver (Grant & Boyd, 2008; 2014).

Now, we discuss some smoothness properties that distinguish KALE from the KL-divergence and which result from the choice of the set of variational functions  $\mathcal{H}$ . Here,  $\mathcal{H}$  doesn't need to contain constant functions. We start by a motivating example in Figure 1, which already illustrates the behavior of KALE relative to KL. This example involves two Gaussians with densities that are reparametrized using a logit-like non-linearity. The slope of the non-linearity is purposely made flatter as the distance between the centers of the Gaussians increases. As a consequence of the invariance of the KL to reparameterization, the flattening doesn't affect the KL which keeps increasing monotonically with

the distance between the centers. While one would expect KALE to behave monotonically w.r.t. KL, the flattening effect leads to a completely different behavior. This also suggests that, while KL might blow up, KALE may still be well-defined. We next show that this is indeed the case, under mild assumptions on  $\mathcal{H}$ , even when  $\mathbb{P}$  doesn't admit a density w.r.t.  $\mathbb{Q}$ . More precisely:

**Proposition 4.** *Assume that functions in  $\mathcal{H}$  have a Lipschitz constant bounded by  $L > 0$  and that  $0 \in \mathcal{H}$ . Then, for any probability distributions  $\mathbb{P}$  and  $\mathbb{Q}$  that admit a first order moment, we have that:*

$$0 \leq \text{KALE}(\mathbb{P} \parallel \mathbb{Q}) \leq LW_1(\mathbb{P}, \mathbb{Q}) < \infty \quad (16)$$

where  $W_1$  is the 1-Wasserstein distance.

We provide a proof of Proposition 4 in Appendix A.2 which simply relies on the convexity of the exponential. (16) implies in particular that for any fixed  $\mathbb{P}$ , the functional  $\mathbb{Q} \mapsto \text{KALE}(\mathbb{P} \parallel \mathbb{Q})$  is continuous w.r.t. the 1-Wasserstein distance at point  $\mathbb{P}$ . An even stronger result holds when  $\mathbb{Q}$  is given as an implicit generative model as in Section 2.2 and when  $\mathcal{H}$  is of the form  $\mathcal{H} = \mathcal{E} + \mathbb{R}$ . In this case, and under additional regularity assumptions on the generator and the energy functions, we show that the function  $\theta \mapsto \text{KALE}(\mathbb{P} \parallel \mathbb{Q}_\theta)$  is *Lipschitz continuous* and *weakly convex*. Lipschitz continuity ensures that KALE is differentiable w.r.t. almost all  $\theta \in \Theta$  by the Rademacher theorem. On the other hand, weak convexity ensures that sub-gradient methods converge to a stationary point (Thekumparmpil et al., 2019; Davis & Drusvyatskiy, 2018) which simply means that there exists some positive constant  $C \geq 0$  such that  $\theta \mapsto \text{KALE}(\mathbb{P} \parallel \mathbb{Q}_\theta) + C\|\theta\|^2$  is convex. This is summarized in Theorem 5, which we prove in Appendix A.2.

**Theorem 5.** *Consider  $\mathcal{H}$  of the form  $\mathcal{H} = \mathcal{E} + \mathbb{R}$ . Under Assumptions (I) to (III), it holds that  $\mathcal{K} : \theta \mapsto \text{KALE}(\mathbb{P} \parallel \mathbb{Q}_\theta)$  is weakly convex, Lipschitz and differentiable for almost all  $\theta \in \Theta$  with a gradient equal to:*

$$\nabla \mathcal{K}(\theta) = \int \nabla_x (f_\theta^* \circ g_\theta) \nabla_\theta g_\theta (p_{f_\theta^*, \theta} \circ g_\theta) d\eta. \quad (17)$$

where  $f_\theta^*$  is a function in  $\mathcal{E}$  that achieves the supremum in (7) and  $p_{f_\theta^*, \theta}$  is the density of the MLE solution w.r.t.  $\mathbb{Q}_\theta$ .

Theorem 5 is motivated by the recent work in (Chu et al., 2020) on the relationship between the stability of GANs during training and the smoothness of the function classes (here the energy functions and the generators). They start from the observation that if a cost function is  $L$ -smooth, i.e. if it has an  $L$ -Lipschitz gradient, then gradient methods converge to a stationary point. This allows them to derive some constraints on the set of discriminators/energies. In our case, we do not require  $L$ -smoothness of KALE, which would be challenging to satisfy. Instead, we only rely on

weak convexity, which is enough for convergence. While this is a weaker requirement, it also leads to conservative convergence rates (Davis & Drusvyatskiy, 2018).

## 4.2. Consistency and convergence rates

In this section, we provide a convergence rate for the estimator in (9) when  $\mathcal{H}$  is an RKHS. The theory remains the same whether  $\mathcal{H}$  contains constants or not. With this choice, the Representer Theorem allows us to reduce the potentially infinite-dimensional optimization problem in (8) to a convex finite-dimensional one. We further restrict ourselves to the *well-specified* case where the density  $r_0$  of  $\mathbb{P}$  w.r.t.  $\mathbb{Q}$  is well-defined and belongs to  $\mathcal{H}$  so that KALE matches the KL. While (Nguyen et al., 2010) (Theorem 3) provides a convergence rate of  $1/\sqrt{N}$  for a related  $M$ -estimator, it requires the density  $r_0$  to be lower-bounded by 0 as well as (generally) upper-bounded. This can be quite restrictive if, for instance,  $r_0$  is the density ratio of two gaussians. In Theorem 6, we provide a similar convergence rate for the estimator defined in (9) without requiring  $r_0$  to be bounded. We provide a proof of this result in Appendix B as well as the full statement of the assumptions.

**Theorem 6.** *Fix any  $1 > \eta > 0$ . Under Assumptions (A) to (C), and provided that  $\lambda = \frac{1}{\sqrt{N}}$ , it holds with probability at least  $1 - 2\eta$  that:*

$$|\widehat{\mathcal{F}}(\hat{h}) - \mathcal{F}(h_0)| \leq \frac{M'(\eta, h_0)}{\sqrt{N}} \quad (18)$$

for a constant  $M'(\eta, h_0)$  that depends only on  $\eta$  and  $h_0$ .

The assumptions in Theorem 6 essentially state that the kernel associated to the RKHS  $\mathcal{H}$  needs to satisfy some integrability requirements. That is to guarantee that the gradient  $\delta \mapsto \nabla \mathcal{F}(h)(\delta)$  and its empirical version are well-defined and continuous. In addition, the optimality condition  $\nabla \mathcal{F}(h) = 0$  is assumed to characterize the global solution  $h_0$ . This will be the case if the kernel is characteristic (Simon-Gabriel & Schölkopf, 2018). The proof of Theorem 6, in Appendix B, takes advantage of the Hilbert structure of the set  $\mathcal{H}$ , the convexity of the functional  $\mathcal{F}$  and the optimality condition  $\nabla \widehat{\mathcal{F}}(\hat{h}) = \lambda \hat{h}$  of the regularized problem, all of which turn out to be sufficient for controlling the error of (9).

## 5. Related work

**Estimation of the KL.** In (Arora et al., 2017), it was shown that estimating the Jensen-Shanon divergence, KL and the Wasserstein distance from finite samples doesn't generalize. This is a consequence of the definition of those divergences which are obtained by solving a functional optimization problem over a large functional space. On the other hand, it was shown that restricting the class of func-

tion to a smaller set, like a parametric set of functions, leads to new divergences which enjoy better generalization properties. We can see from Theorem 6 that KALE falls into this category of divergences. When the density between two probability distributions happens to be in that class of functions, then KALE matches KL, therefore making the estimation of the KL possible for those particular probability distributions.

**Fenchel Duality for unnormalized density estimation.** (Dai et al., 2019a;b) consider the task of MLE using an infinite-dimensional set of energies. They propose to use a dual formulation for the intractable log-partition function by expressing it as a supremum over probability distributions of some concave cost functional (Wainwright & Jordan, 2008). The MLE problem is then written as a minimax problem which can be approximately solved by alternating optimization over the energy functions and a restricted class of probability distributions. This is unlike our approach in Section 3.1, which only requires to maximize (6) for estimating the maximum likelihood. (Gutmann & Hyvärinen, 2012) introduced an additional parameter  $c$  to learn the intractable partition function as well as the energy  $f$ . The augmented model  $h = f + c$  was then learned using a classification loss between the data distribution and a fixed proposal distribution. This choice of loss was motivated after observing that maximum likelihood on the augmented model without accounting for the normalizer leads to an ill-defined objective that systematically blows up. Instead, we propose to use the augmented model for optimizing the lower bound (6) which is always well-defined as shown in Proposition 1. Hence, we can directly perform MLE on unnormalized models.

**Sampling using the discriminator.** Recent work proposes using the discriminator of a GAN for rejection sampling (Azadi et al., 2019) or Metropolis-Hastings correction (Turner et al., 2019) using the generator as a proposal distribution. The motivation is that a discriminator trained using the standard GAN loss approximates the log-density ratio between the target and the generator/base distribution. This requires the data distribution to admit a density w.r.t. the generator. Moreover, sampling is performed directly on the high-dimensional input space without further taking into account the lower-dimensional structure of the generator and without using gradient information provided by the discriminator. (Ding et al., 2019) introduce a different loss for density ratio estimation and propose to use it in a sampling algorithm performed on some feature space of an auxiliary pre-trained network. The sampling procedure is then extended to methods like sampling-importance resampling (Bol, 2005) but is still agnostic to the structure of the generator. In a different line of work, (Lawson et al., 2019) propose to treat the sampling procedure as a model

of interest which is then learned by maximizing the ELBO.

**Latent space optimization for IGMs.** Methods to optimize over the latent space were recently considered, as opposed to Section 3.2 which samples from the latent noise according to a learned energy model. (Wu et al., 2019b) is motivated by the compressed sensing framework (Donoho, 2006; Candès et al., 2006), where the latent noise is optimized during training to minimize a measurement error. This optimized noise is then used to train the generator instead of the randomly sampled noise. The discriminator is trained to minimize a Restricted Isometry Property, thus preventing the generator from collapsing to a trivial solution. In a follow-up work, (Wu et al., 2019a) improves the method using the natural gradient and achieves state-of-the-art results on high resolution image generation. Finally, (Tanaka, 2019) adopts an optimal transport point of view where a deterministic optimal transport map between the generator and the data distribution is estimated, assuming its existence. The transport map is then used to compute optimized samples from the latent space. This is in contrast to the latent space diffusion considered in the present work.

## 6. Experiments

### 6.1. Energy based learning

To illustrate the effectiveness of KALE for performing MLE on energy-based models, we consider the task of density estimation on five UCI datasets (Dheeru & Taniskidou, 2017) using the same experimental setup as in (Wenliang et al., 2019) and compare EBMs trained using KALE with 6 other methods: (DKEF (Wenliang et al., 2019), MADE (Germain et al., 2015), MAF/MAF-MOG (Papamakarios et al., 2017) and NVP (Dinh et al., 2016)). All those methods, except DKEF, have a closed form likelihood and can therefore be maximized by direct optimization. We use an EBM where the energy function is parameterized by a network with 3 hidden layers and  $10^3$  units per layer. For the base distribution, we use a MADE network (Germain et al., 2015) with 3 autoregressive hidden layers, each one of them having  $10^3$  units. In order to ensure that the base distribution is well aligned with the data, we optimize its parameters by maximizing the likelihood. Once the base model is optimized, we learn the energy models by maximizing the objective (6). For the regularization  $I(f + c)$ , we use a combination of  $L_2$  norm and a variant of the gradient penalty (Gulrajani et al., 2017). We also use a preconditioning for the gradient as proposed in (Şimşekli et al., 2020) to stabilize training and avoid taking large noisy step-sizes due to the exponential term. More details about the experiments can be found in Appendix D. Table 1 shows the negative log-likelihood on the test set for each method. For KALE, we consider the model that achieves the best performance on the validation

Method	RedWine	WhiteWine	Parkinsons	HepMass	MiniBoone
KALE	$12.41 \pm 0.03$	<b><math>12.87 \pm 0.08</math></b>	<b><math>12.08 \pm 0.04</math></b>	$22.77 \pm 0.11$	$41.92 \pm 0.16$
DKEF	$12.41 \pm 0.13$	$13.43 \pm 0.09$	$14.02 \pm 0.16$	$28.15 \pm 1.35$	$40.83 \pm 1.05$
MADE	$13.93 \pm 0.61$	$14.34 \pm 0.29$	$14.44 \pm 0.19$	$29.99 \pm 0.23$	$55.82 \pm 0.17$
MAF	$13.94 \pm 0.2$	$14.38 \pm 0.14$	$13.39 \pm 0.08$	$23.94 \pm 0.04$	$40.35 \pm 0.14$
MAF-MOG	$12.39 \pm 0.11$	$13.36 \pm 0.15$	$12.86 \pm 0.07$	$19.39 \pm 0.05$	<b><math>35.4 \pm 0.1</math></b>
NVP	<b><math>12.14 \pm 0.08</math></b>	<b><math>12.87 \pm 0.06</math></b>	$12.19 \pm 0.06$	<b><math>17.96 \pm 0.06</math></b>	<b><math>35.54 \pm 0.1</math></b>

Table 1: UCI datasets: average and standard deviation of the negative log-likelihood over 15 different runs computed on the test set and for 7 different methods for density estimation. Best method in boldface. For KALE, a lower-bound on the likelihood is computed according to Proposition 1.

set and report the variational lower-bound on log-likelihood in Proposition 1 evaluated on the test set. All numerical results for the remaining methods were provided by authors of (Wenliang et al., 2019) upon request. The first remark is that using the EBM model trained on KALE with a base provided by a pre-trained MADE improves the likelihood over simply using MADE, suggesting that both models learn complementary information about the data. The proposed approach often outperforms DKEF for which the likelihood is also intractable and, in most cases, performs as well as the remaining models for which the likelihood can be evaluated in closed form.

## 6.2. Sampling from an Implicit EBM

In this section, we provide empirical evidence that the energy model can improve the quality of the samples obtained from a generator after performing Langevin Monte Carlo on the latent space as described in Section 3.2. Prior work (Nowozin et al., 2016) has already shown empirically that using the variational objective (6) to train implicit models in an adversarial setting yields comparable results to other losses. Thus, we only focus on the case where the generator is already pre-trained to produce descent samples. We consider the task of unsupervised image generation on CIFAR-10 dataset (Krizhevsky, 2009). We use a pre-trained DCGAN generator (Radford et al., 2016) as a base distribution. The latent noise is generated from a standard Gaussian distribution of dimension 100. For the energy function/discriminator, we consider the following networks: DCGAN, DCGAN with spectral norm (DCGAN-SN), DCGAN-SN with gradient penalty (DCGAN-SN-GP) and ResNet-SN-GP. We train the energy models using Algorithm 1, and then use Algorithm 2 for sampling and evaluate the quality of the generated samples using the FID scores (Heusel et al., 2017) computed on  $5 \times 10^4$  generated samples. Full details of the experiments are provided in Appendix D. Table 2 shows both the  $\mathbb{Q}$ -log-likelihood and FID scores of the EBMs.

The first observation is that all samples obtained from the EBMs have lower FID scores than the samples obtained

using the generator only. Figures 2a and 2b of Appendix D seem to confirm this improvement visually. The second observation is that using a larger network (ResNet) improves the sample quality over a smaller one (DCGAN). Interestingly, for SCGAN, using both SN and GP leads to a drop in performance over using SN only. We also noticed during sampling that sudden phase transitions happen in which images shift from one object to another and within a short time window all images become uniform noise. We hypothesize that this is due to the nature of the sampler which constructs a chain that explores high density regions in a continuous way, hence sometimes traversing low-density regions.

	$\mathbb{Q}$ -log-likelihood	FID
Base	0	$35.9$
DCGAN	$1.0$	$34.0 \pm .01$
DCGAN-SN	$4.13$	$33.2 \pm .03$
DCGAN-SN-GP	$3.11$	$33.7 \pm .12$
ResNet-SN-GP	$0.23$	$33.2 \pm .09$

Table 2: Unsupervised image generation on CIFAR-10. The generalized log-likelihood w.r.t. to the fixed generator and FID scores are reported. Four different energy models are compared to the generator (Base).

## References

Resampling algorithms and architectures for distributed particle filters. *IEEE Transactions on Signal Processing*, 53(7):2442–2450, July 2005.

Arbel, M. and Gretton, A. Kernel Conditional Exponential Family. In *International Conference on Artificial Intelligence and Statistics*, pp. 1337–1346, March 2018. URL <http://proceedings.mlr.press/v84/arbel18a.html>.

Arjovsky, M., Chintala, S., and Bottou, L. Wasserstein generative adversarial networks. In *Proceedings of the 34th International Conference on Machine Learning*, volume 70 of *Proceedings of Ma-*

chine Learning Research, pp. 214–223, International Convention Centre, Sydney, Australia, 06–11 Aug 2017. PMLR. URL <http://proceedings.mlr.press/v70/arjovsky17a.html>.

Arora, S., Ge, R., Liang, Y., Ma, T., and Zhang, Y. Generalization and equilibrium in generative adversarial nets (GANs). In *Proceedings of the 34th International Conference on Machine Learning*, volume 70 of *Proceedings of Machine Learning Research*, pp. 224–232. PMLR, 06–11 Aug 2017. URL <http://proceedings.mlr.press/v70/arora17a.html>.

Azadi, S., Olsson, C., Darrell, T., Goodfellow, I., and Odena, A. Discriminator rejection sampling. In *International Conference on Learning Representations*, 2019. URL <https://openreview.net/forum?id=S1GkToR5tm>.

Bińkowski, M., Sutherland, D. J., Arbel, M., and Gretton, A. Demystifying MMD GANs. In *International Conference on Learning Representations*, 2018. URL <https://openreview.net/forum?id=r11UOzWCW>.

Bottou, L., Arjovsky, M., Lopez-Paz, D., and Oquab, M. Geometrical insights for implicit generative modeling. In *Braverman Readings in Machine Learning*, 2017.

Candès, E., Romberg, J., and Tao, T. Stable signal recovery from incomplete and inaccurate measurements. *Communications on Pure and Applied Mathematics*, 59, 08 2006.

Canu, S. and Smola, A. Kernel methods and the exponential family. *Neurocomput.*, 69(7–9):714–720, March 2006. URL <http://dx.doi.org/10.1016/j.neucom.2005.12.009>.

Chu, C., Minami, K., and Fukumizu, K. Smoothness and stability in gans. In *International Conference on Learning Representations*, 2020. URL <https://openreview.net/forum?id=HJeOekHKwr>.

Dai, B., Dai, H., Gretton, A., Song, L., Schuurmans, D., and He, N. Kernel exponential family estimation via doubly dual embedding. In *Proceedings of Machine Learning Research*, volume 89 of *Proceedings of Machine Learning Research*, pp. 2321–2330. PMLR, 16–18 Apr 2019a. URL <http://proceedings.mlr.press/v89/dai19a.html>.

Dai, B., Liu, Z., Dai, H., He, N., Gretton, A., Song, L., and Schuurmans, D. Exponential Family Estimation via Adversarial Dynamics Embedding. *arXiv:1904.12083 [cs, stat]*, December 2019b. URL <http://arxiv.org/abs/1904.12083>. arXiv: 1904.12083.

Davis, D. and Drusvyatskiy, D. Stochastic subgradient method converges at the rate  $\mathcal{O}(k^{-1/4})$  on weakly convex functions. *arXiv:1802.02988 [cs, math]*, February 2018. URL <http://arxiv.org/abs/1802.02988>.

Dheeru, D. and Taniskidou, E. K. Uci machine learning repository, 2017. URL <http://archive.ics.uci.edu/ml>.

Ding, X., Wang, Z. J., and Welch, W. J. Subsampling Generative Adversarial Networks: Density Ratio Estimation in Feature Space with Softplus Loss. 2019. URL <http://arxiv.org/abs/1909.10670>.

Dinh, L., Sohl-Dickstein, J., and Bengio, S. Density estimation using real nvp. 05 2016. URL <https://arxiv.org/abs/1605.08803>.

Donoho, D. L. Compressed sensing. *IEEE Transactions on Information Theory*, 52(4):1289–1306, April 2006. ISSN 1557-9654.

Du, Y. and Mordatch, I. Implicit generation and modeling with energy based models. In *Advances in Neural Information Processing Systems 32*, pp. 3608–3618. Curran Associates, Inc., 2019. URL <https://arxiv.org/abs/1903.08689>.

Eberle, A., Guillin, A., and Zimmer, R. Couplings and quantitative contraction rates for Langevin dynamics. *The Annals of Probability*, 2017. URL <http://arxiv.org/abs/1703.01617>.

Ekeland, I. and Témam, R. *Convex Analysis and Variational Problems*. Classics in Applied Mathematics. Society for Industrial and Applied Mathematics, 01 1999. URL <https://epubs.siam.org/doi/book/10.1137/1.9781611971088>.

Fukumizu, K. Exponential manifold by reproducing kernel Hilbert spaces, October 2009.

Germain, M., Gregor, K., Murray, I., and Larochelle, H. MADE: Masked autoencoder for distribution estimation. *ICML*, 2015. URL <http://arxiv.org/abs/1502.03509>.

Goodfellow, I., Pouget-Abadie, J., Mirza, M., Xu, B., Warde-Farley, D., Ozair, S., Courville, A., and Bengio, Y. Generative adversarial nets. In *Advances in Neural Information Processing Systems 27*, pp. 2672–2680. Curran Associates, Inc., 2014. URL <http://papers.nips.cc/paper/5423-generative-adversarial-nets.pdf>.

Grant, M. and Boyd, S. Graph implementations for nonsmooth convex programs. In *Recent Advances in Learning*

and Control, Lecture Notes in Control and Information Sciences, pp. 95–110. Springer-Verlag Limited, 2008.

Grant, M. and Boyd, S. CVX: Matlab software for disciplined convex programming, version 2.1. <http://cvxr.com/cvx>, March 2014.

Grover, A., Song, J., Kapoor, A., Tran, K., Agarwal, A., Horvitz, E. J., and Ermon, S. Bias correction of learned generative models using likelihood-free importance weighting. In *Advances in Neural Information Processing Systems 32*, pp. 11058–11070. Curran Associates, Inc., 2019. URL <https://arxiv.org/abs/1906.09531>.

Gulrajani, I., Ahmed, F., Arjovsky, M., Dumoulin, V., and Courville, A. Improved training of wasserstein gans. In *Proceedings of the 31st International Conference on Neural Information Processing Systems, NIPS’17*, pp. 5769–5779, Red Hook, NY, USA, 2017. Curran Associates Inc. ISBN 9781510860964.

Gutmann, M. U. and Hyvärinen, A. Noise-contrastive estimation of unnormalized statistical models, with applications to natural image statistics. *The Journal of Machine Learning Research*, 13(null):307–361, February 2012.

Heusel, M., Ramsauer, H., Unterthiner, T., Nessler, B., and Hochreiter, S. Gans trained by a two time-scale update rule converge to a local nash equilibrium. In *Advances in Neural Information Processing Systems 30*, pp. 6626–6637. Curran Associates, Inc., 2017. URL <https://arxiv.org/abs/1706.08500>.

Hinton, G. E. Training products of experts by minimizing contrastive divergence. *Neural Computation*, 14(8):1771–1800, August 2002. ISSN 0899-7667. URL <https://doi.org/10.1162/089976602760128018>.

Hyvärinen, A. Estimation of Non-Normalized Statistical Models by Score Matching. *The Journal of Machine Learning Research*, 6:695–709, December 2005. ISSN 1532-4435. URL <http://dl.acm.org/citation.cfm?id=1046920.1088696>.

Jordan, M. I., Ghahramani, Z., Jaakkola, T. S., and Saul, L. K. An introduction to variational methods for graphical models. In *Learning in graphical models*, pp. 105–161. MIT Press, Cambridge, MA, USA, February 1999. ISBN 978-0-262-60032-3.

Kingma, D. P. and Welling, M. Auto-encoding variational Bayes. *ICLR*, 2014.

Krizhevsky, A. Learning multiple layers of features from tiny images. Technical report, University of Toronto, 2009.

Lawson, J., Tucker, G., Dai, B., and Ranganath, R. Energy-inspired models: Learning with sampler-induced distributions. In *Advances in Neural Information Processing Systems 32*, pp. 8501–8513. Curran Associates, Inc., 2019. URL <https://arxiv.org/abs/1910.14265>.

LeCun, Y., Chopra, S., Hadsell, R., Ranzato, M., and Huang, F.-J. *Predicting Structured Data*, chapter A Tutorial on Energy-Based Learning. MIT Press, 2006.

Li, C.-L., Chang, W.-C., Cheng, Y., Yang, Y., and Poczos, B. Mmd gan: Towards deeper understanding of moment matching network. In *Advances in Neural Information Processing Systems 30*, pp. 2203–2213. Curran Associates, Inc., 2017. URL <https://arxiv.org/abs/1705.08584>.

Milgrom, P. and Segal, I. Envelope Theorems for Arbitrary Choice Sets. *Econometrica*, 70(2):583–601, 2002. ISSN 1468-0262. URL <https://onlinelibrary.wiley.com/doi/abs/10.1111/1468-0262.00296>.

Miyato, T., Kataoka, T., Koyama, M., and Yoshida, Y. Spectral normalization for generative adversarial networks. In *International Conference on Learning Representations*, 2018. URL <https://openreview.net/forum?id=B1QRgziT->.

Nguyen, X., Wainwright, M. J., and Jordan, M. I. Estimating divergence functionals and the likelihood ratio by convex risk minimization. *IEEE Transactions on Information Theory*, 56(11):5847–5861, 2010.

Nowozin, S., Cseke, B., and Tomioka, R. f-gan: Training generative neural samplers using variational divergence minimization. In *Advances in Neural Information Processing Systems 29*, pp. 271–279. Curran Associates, Inc., 2016. URL <https://arxiv.org/abs/1606.00709>.

Papamakarios, G., Pavlakou, T., and Murray, I. Masked autoregressive flow for density estimation. *NIPS*, 2017. URL <http://arxiv.org/abs/1705.07057>.

Radford, A., Metz, L., and Chintala, S. Unsupervised representation learning with deep convolutional generative adversarial networks. In *4th International Conference on Learning Representations, ICLR 2016, San Juan, Puerto Rico, May 2-4, 2016, Conference Track Proceedings*, 2016. URL <http://arxiv.org/abs/1511.06434>.

Rutherford, J. R. Review: J. diestel and j. j. uhl, jr., vector measures. *Bull. Amer. Math. Soc.*, 84(4):681–685, 07 1978. URL <http://projecteuclid.org/euclid.bams/1183540941>.

Rezende, D. J., Mohamed, S., and Wierstra, D. Stochastic backpropagation and approximate inference in deep generative models. In *ICML*, pp. 1278–1286, 2014.

Rockafellar, R. T. *Convex analysis*. Princeton Mathematical Series. Princeton University Press, Princeton, N. J., 1970.

Sachs, M., Leimkuhler, B., and Danos, V. Langevin Dynamics with Variable Coefficients and Nonconservative Forces: From Stationary States to Numerical Methods. *Entropy*, 19(12):647, December 2017. URL <https://www.mdpi.com/1099-4300/19/12/647>.

Sanjabi, M., Ba, J., Razaviyayn, M., and Lee, J. D. On the convergence and robustness of training gans with regularized optimal transport. In *Advances in Neural Information Processing Systems 31*, pp. 7091–7101. Curran Associates, Inc., 2018. URL <https://arxiv.org/abs/1802.08249>.

Simon-Gabriel, C.-J. and Schölkopf, B. Kernel distribution embeddings: Universal kernels, characteristic kernels and kernel metrics on distributions. *Journal of Machine Learning Research*, 19(44):1–29, 2018. URL <http://jmlr.org/papers/v19/16-291.html>.

Şimşekli, U., Zhu, L., Teh, Y. W., and Gürbüzbalaban, M. Fractional Underdamped Langevin Dynamics: Retargeting SGD with Momentum under Heavy-Tailed Gradient Noise. *arXiv:2002.05685 [cs, stat]*, February 2020. URL <http://arxiv.org/abs/2002.05685>. arXiv: 2002.05685.

Sriperumbudur, B., Fukumizu, K., Kumar, R., Gretton, A., and Hyvärinen, A. Density estimation in infinite dimensional exponential families. *Journal of Machine Learning Research*, 12 2017. URL <https://arxiv.org/abs/1312.3516>.

Sturm, K. T. Diffusion processes and heat kernels on metric spaces. *The Annals of Probability*, 26(1):1–55, January 1998. ISSN 0091-1798, 2168-894X. URL <https://projecteuclid.org/euclid.aop/1022855410>.

Sutherland, D., Strathmann, H., Arbel, M., and Gretton, A. Efficient and principled score estimation with Nyström kernel exponential families. In *International Conference on Artificial Intelligence and Statistics*, pp. 652–660, March 2018. URL <http://proceedings.mlr.press/v84/sutherland18a.html>.

Tanaka, A. Discriminator optimal transport. In *Advances in Neural Information Processing Systems 32*, pp. 6813–6823. Curran Associates, Inc., 2019. URL <http://papers.nips.cc/paper/8906-discriminator-optimal-transport.pdf>.

Thekumparampil, K. K., Jain, P., Netrapalli, P., and Oh, S. Efficient algorithms for smooth minimax optimization. In *Advances in Neural Information Processing Systems 32*, pp. 12680–12691. Curran Associates, Inc., 2019. URL <http://arxiv.org/abs/1907.01543>.

Turner, R., Hung, J., Frank, E., Saatchi, Y., and Yosinski, J. Metropolis-Hastings generative adversarial networks. In *Proceedings of the 36th International Conference on Machine Learning*, volume 97 of *Proceedings of Machine Learning Research*, pp. 6345–6353, Long Beach, California, USA, 09–15 Jun 2019. PMLR. URL <http://proceedings.mlr.press/v97/turner19a.html>.

Wainwright, M. J. and Jordan, M. I. Graphical Models, Exponential Families, and Variational Inference. *Foundations and Trends® in Machine Learning*, 1(1–2):1–305, November 2008. URL <https://www.nowpublishers.com/article/Details/MAL-001>.

Wenliang, L., Sutherland, D., Strathmann, H., and Gretton, A. Learning deep kernels for exponential family densities. In *International Conference on Machine Learning*, pp. 6737–6746, May 2019. URL <http://proceedings.mlr.press/v97/wenliang19a.html>.

Wu, Y., Donahue, J., Balduzzi, D., Simonyan, K., and Lillicrap, T. LOGAN: Latent Optimisation for Generative Adversarial Networks. *arXiv:1912.00953 [cs, stat]*, December 2019a. URL <http://arxiv.org/abs/1912.00953>. arXiv: 1912.00953.

Wu, Y., Rosca, M., and Lillicrap, T. Deep compressed sensing. In *Proceedings of the 36th International Conference on Machine Learning*, volume 97 of *Proceedings of Machine Learning Research*, pp. 6850–6860, Long Beach, California, USA, 09–15 Jun 2019b. PMLR. URL <http://proceedings.mlr.press/v97/wu19d.html>.

## A. Latent noise sampling and Smoothness of KALE

We begin by stating the assumptions that will be used in this section:

(I)  $\mathcal{E}$  is parametrized by a compact set of parameters  $\Psi$  and any  $f \in \mathcal{E}$  is continuous w.r.t those parameters.

(II) Functions in  $\mathcal{E}$  are jointly continuous w.r.t.  $(\psi, x)$  and are  $L$ -lipschitz and  $L$ -smooth w.r.t. to the input  $x$ :

$$\|f_\psi(x) - f_\psi(x')\| \leq L\|x - x'\|, \quad (19)$$

$$\|\nabla_x f_\psi(x) - \nabla_x f_\psi(x')\| \leq L\|x - x'\| \quad (20)$$

(III) There exists a square integrable function  $a : \mathcal{Z} \mapsto \mathbb{R}$  and an integrable function  $b : \mathcal{Z} \mapsto \mathbb{R}$  such that generators  $\theta \mapsto g_\theta(z)$  are  $a$ -Lipschitz and  $b$ -smooth in the following sense:

$$\|g_\theta(z) - g_{\theta'}(z)\| \leq |a(z)|\|\theta - \theta'\| \quad (21)$$

$$\|\nabla_\theta g_\theta(z) - \nabla_\theta g_{\theta'}(z)\| \leq |b(z)|\|\theta - \theta'\|. \quad (22)$$

Moreover, for all  $h \in \mathcal{E}$  and  $\theta \in \Theta$  the square integral of  $a$  and integral of  $b$  are uniformly bounded by some constant  $C$ .

$$\int |a(z)|^2 p_{h,\theta} \circ g_\theta d\eta \leq C \quad (23)$$

$$\int |b(z)| p_{h,\theta} \circ g_\theta d\eta \leq C \quad (24)$$

(IV) The generator is  $L$ -Lipschitz and  $L$ -smooth w.r.t. to the input  $z$  for all  $\theta \in \Theta$ :

$$|g_\theta(z) - g_\theta(z')| \leq L\|z - z'\|, \quad (25)$$

$$\|\nabla_z g_\theta(z) - \nabla_z g_\theta(z')\| \leq L\|z - z'\|. \quad (26)$$

### A.1. Latent space sampling

Here we prove Proposition 3 which only relies on Assumptions (II) and (IV).

*Proof of Proposition 3.* Let  $\pi_t$  be the probability distribution of  $(z_t, v_t)$  at time  $t$  of the diffusion in (14), which we recall here:

$$\begin{aligned} dz_t &= v_t dt \\ dv_t &= -(\kappa v_t + \nabla U(z_t)) + \sqrt{2\kappa} dw_t, \end{aligned} \quad (27)$$

We call  $\pi_\infty$  its corresponding invariant distribution given by:

$$\pi_\infty(z, v) \propto \exp -U(z) - \frac{1}{2}\|v\|^2 \quad (28)$$

By Assumptions (II) and (IV) it is easy to see that  $U$  is bounded from below and has Lipschitz gradient. Moreover, by Lemma 7 we know that  $U$  is also dissipative. This allows to directly apply (Eberle et al., 2017)(Corollary 2.6.) which implies that:

$$W_2(\pi_t, \pi_\infty) \leq C_1 \exp(-tc) \quad (29)$$

where  $c$  is a positive constant and  $C_1$  only depends on  $\pi_\infty$  and the initial distribution  $\pi_0$ . Now we consider an optimal coupling  $\Pi_t$  between  $\pi_t$  and  $\pi_0$ . Given joints samples  $((z_t, v_t), (z, v))$  from  $\Pi_t$ , we consider the following samples in input space  $(x_t, x) := (g_{\theta^*}(z_t), g_{\theta^*}(z))$ . Since  $z_t$  and  $z$  has marginals  $p_{it}$  and  $p_{i\infty}$ , it is easy to see that  $x_t \sim \mathbb{P}_t$  and  $x \sim \mathbb{P}_{f^*, \mathbb{Q}_{\theta^*}}$ . Therefore, by definition of the  $W_2$  distance, we have the following bound:

$$W_2^2(\mathbb{P}_t, \mathbb{P}_{f^*, \mathbb{Q}_{\theta^*}}) \leq \mathbb{E} [\|x_t - x\|^2] \quad (30)$$

$$\leq \int \|g_{\theta^*}(z_t) - g_{\theta^*}(z)\|^2 d\Pi_t(z_t, z) \quad (31)$$

$$\leq L^2 \int \|z_t - z\|^2 d\Pi_t(z_t, z) \quad (32)$$

$$\leq L^2 W_2^2(\pi_t, \pi_\infty) \leq C_1 L^2 \exp(-tc). \quad (33)$$

The second line uses the finition of  $(x_t, x)$  as joint samples obtained using  $(z_t, z)$ . The third line uses the assumption that  $g_{\theta^*}$  is  $L$ Lipschitz, finally the last line uses that  $\Pi_t$  is an optimal coupling between  $\pi_t$  and  $\pi_\infty$ .  $\square$

**Lemma 7.** *Under Assumptions (II) and (IV), there exists  $A > 0$  and  $\lambda \in (0, \frac{1}{4}]$  such that:*

$$\frac{1}{2} z^\top \nabla U(z) \geq \lambda \left( U(z) + \frac{\gamma^2}{4} \|z\|^2 \right) - A \quad (34)$$

for all  $z \in \mathcal{Z}$ .

*Proof.* For simplicity, let's call  $w(z) = f^* \circ g_{\theta^*}(z)$  and denote by  $M$  an upper-bound on the Lipschitz constant of  $w$  and  $\nabla w$  which is guaranteed to be finite. Hence  $U(z) = \frac{1}{2}\|z\|^2 + w(z)$ . Equation (34) is equivalent to having:

$$\left( 1 - \lambda \left( 1 + \frac{\gamma^2}{2} \right) \right) \|z\|^2 \geq 2\lambda w(z) - z^\top \nabla w(z) - A \quad (35)$$

Using that  $w$  is Lipschitz, we have that  $w(z) \leq w(0) + M\|z\|$  and  $-z^\top \nabla w(z) \leq M\|z\|$ . Hence, a sufficient condition for (35) to hold is to have:

$$\left( 1 - \lambda \left( 1 + \frac{\gamma^2}{2} \right) \right) \|z\|^2 - (2\lambda + 1)M\|z\| + A \geq 0 \quad (36)$$

The l.h.s. in the above equation is a quadratic function in  $\|z\|$  and admits a global minimum as soon as  $\lambda < (1 + \frac{\gamma^2}{2})^{-1}$ . Moreover, the global minimum is always positive provided that  $A$  is large enough.  $\square$

## A.2. Smoothness of KALE

*Proof of Proposition 4.* For any  $h \in \mathcal{H}$  the following holds:

$$\mathcal{F}(h) = - \int h d\mathbb{P} - \int \exp(-h) d\mathbb{Q} + 1 \quad (37)$$

$$= \int h(x) - h(x') d\mathbb{Q}(x) d\mathbb{P}(x') \quad (38)$$

$$- \int \underbrace{(\exp(-h) + h - 1)}_{\geq 0} d\mathbb{Q} \quad (39)$$

$$\leq \int h(x) - h(x') d\mathbb{Q}(x) d\mathbb{P}(x') \leq LW_1(\mathbb{P}, \mathbb{Q}) \quad (40)$$

The first inequality results from the convexity of  $\exp$  while the last one is a consequence of  $h$  being  $L$ -Lipschitz. This allows to conclude that  $KALE(\mathbb{P}||\mathbb{Q}) \leq LW_1(\mathbb{P}, \mathbb{Q})$  after taking the supremum over all  $h \in \mathcal{H}$ .  $\square$

Here, to simplify notations, we will denote by  $\mathcal{L}_\theta(f)$ , the expected  $\mathbb{Q}_\theta$  log-likelihood under  $\mathbb{P}$ . In other words:

$$\mathcal{L}_\theta(f) := \mathcal{L}_{\mathbb{Q}_\theta}(f, \mathbb{P}) = - \int f d\mathbb{P} - \log \int \exp(-f) d\mathbb{Q}_\theta. \quad (41)$$

We also denote by  $p_{f,\theta}$  the density of the model w.r.t.  $\mathbb{Q}_\theta$ :

$$p_{f,\theta} = \frac{\exp(-f)}{Z_\theta(f)}, \quad Z_\theta(f) = \int \exp(-f) d\mathbb{Q}_\theta. \quad (42)$$

Moreover, we write  $\mathcal{K}(\theta) := KALE(\mathbb{P}||\mathbb{Q}_\theta)$  to emphasize the dependence on  $\theta$ .

*Proof of Theorem 5.* We will first prove that  $\theta \mapsto \mathcal{K}(\theta)$  is weakly convex in  $\theta$ . By Lemma 8, we know that  $\theta \mapsto \mathcal{L}_\theta(f)$  is  $M$ -smooth for some positive constant  $M$ , this directly implies that it is also weakly convex. Therefore, the following inequality holds:

$$\mathcal{L}_{\theta_t}(f) \leq t\mathcal{L}_\theta(f) + (1-t)\mathcal{L}_{\theta'}(f) + \frac{M}{2}t(1-t)\|\theta - \theta'\|^2. \quad (43)$$

Taking the supremum w.r.t.  $f$ , it follows that:

$$\mathcal{K}(\theta_t) \leq t\mathcal{K}(\theta) + (1-t)\mathcal{K}(\theta') + \frac{M}{2}t(1-t)\|\theta - \theta'\|^2. \quad (44)$$

This precisely means that  $K$  is weakly convex in  $\theta$ .

To prove that it is Lipschitz, we will also use Lemma 8 which states that  $\mathcal{L}_\theta(f)$  is Lipschitz in  $\theta$  uniformly on  $\mathcal{E}$ . Hence, the following holds:

$$\mathcal{L}_\theta(f) \leq \mathcal{L}_\theta(f) + LC\|\theta - \theta'\| \quad (45)$$

Again, taking the supremum over  $f$ , it follows directly:

$$\mathcal{K}(\theta) \leq \mathcal{K}(\theta') + LC\|\theta - \theta'\| \quad (46)$$

One concludes that  $\mathcal{K}$  is Lipschitz by exchanging the roles of  $\theta$  and  $\theta'$  to get the other side of the inequality. Hence, by Rademacher theorem,  $\mathcal{K}$  is differentiable for almost all  $\theta$ .

We will now provide an expression for the gradient of  $\mathcal{K}$ . Recall that, by Assumption (I), any function  $f \in \mathcal{E}$  is continuous w.r.t. the parameters of  $\mathcal{E}$  which are also compact. Hence, by continuity of  $\mathcal{L}_\theta(f)$  w.r.t.  $f$  it is easy to see that the supremum  $\sup_{f \in \mathcal{E}} \mathcal{L}_\theta(f)$  is achieved for some function  $f_\theta^*$ . Moreover, we know that  $\mathcal{L}_\theta(f)$  is smooth uniformly on  $\mathcal{E}$ , therefore, the family  $(\partial_\theta \mathcal{L}_\theta(f))_{f \in \mathcal{E}}$  is equi-differentiable. We are in position to apply (Milgrom & Segal, 2002)(Theorem 3) which ensures that  $\mathcal{K}(\theta)$  admits left and right partial derivatives given by:

$$\begin{aligned} \partial_e^+ \mathcal{K}(\theta) &= \lim_{\substack{t > 0 \\ t \rightarrow 0}} \partial_\theta \mathcal{L}_\theta(f_{\theta+te}^*)^\top e \\ \partial_e^- \mathcal{K}(\theta) &= \lim_{\substack{t < 0 \\ t \rightarrow 0}} \partial_\theta \mathcal{L}_\theta(f_{\theta+te}^*)^\top e, \end{aligned} \quad (47)$$

where  $e$  is a given direction in  $\mathbb{R}^r$ . Moreover, the theorem also states that  $\mathcal{K}(\theta)$  is differentiable iff  $t \mapsto f_{\theta+te}^*$  is continuous at  $t = 0$ . Now, recalling that  $\mathcal{K}(\theta)$  is actually differentiable for almost all  $\theta$ , it must hold that  $f_{\theta+te}^* \rightarrow_{t \rightarrow 0} f_\theta^*$  and  $\partial_e^+ \mathcal{K}(\theta) = \partial_e^- \mathcal{K}(\theta)$  for almost all  $\theta$ . This implies that the two limits in (47) are actually equal to  $\partial_\theta \mathcal{L}_\theta(f_\theta^*)^\top e$ . The gradient of  $\mathcal{K}$ , whenever defined, is therefore given by:

$$\nabla_\theta \mathcal{K}(\theta) = \int ((\nabla_x f_\theta^* \circ g_\theta) \nabla_\theta g_\theta) (p_{f_\theta^*, \theta} \circ g_\theta) d\eta. \quad (48)$$

$\square$

**Lemma 8.** *Under Assumptions (I) to (III), the functional  $\mathcal{L}_\theta(f)$  is Lipschitz and smooth in  $\theta$  uniformly on  $\mathcal{E}$ :*

$$|\mathcal{L}_\theta(f) - \mathcal{L}_{\theta'}(f)| \leq LC\|\theta - \theta'\| \quad (49)$$

$$\|\partial_\theta \mathcal{L}_\theta(f) - \partial_\theta \mathcal{L}_{\theta'}(f)\| \leq 2CL(1+L)\|\theta - \theta'\| \quad (50)$$

*Proof.* By the dominated convergence theorem allows it is easy to see that  $\mathcal{L}_\theta(f)$  is differentiable and that:

$$\partial_\theta \mathcal{L}_\theta(f) := \int (\nabla_x f \circ g_\theta) \nabla_\theta g_\theta (p_{f,\theta} \circ g_\theta) d\eta \quad (51)$$

Hence, it is easy to see that  $\partial_\theta \mathcal{L}_\theta(f)$  is bounded since  $f$  and  $g_\theta$  are Lipschitz in  $x$  and  $\theta$  respectively. More precisely, we have that:

$$\|\partial_\theta \mathcal{L}_\theta(f)\| \leq L \int |a| p_{f,\theta} \circ g_\theta \leq LC. \quad (52)$$

This implies in particular that  $\mathcal{L}_\theta(f)$  is Lipschitz with a constant  $LC$ . Now we will show that it is also smooth. For this, we need to control the difference

$$D := \|\partial_\theta \mathcal{L}_\theta(f) - \partial_\theta \mathcal{L}_{\theta'}(f)\|$$

. We have by triangular inequality:

$$D \leq \underbrace{\int \|\nabla_x f \circ g_\theta - \nabla_x f \circ g_{\theta'}\| \|\nabla_\theta g_\theta\| (p_{f,\theta} \circ g_\theta) d\eta}_I \quad (53)$$

$$+ \underbrace{\int \|\nabla_x f \circ g_\theta\| \|\nabla_\theta g_\theta - \nabla_\theta g_{\theta'}\| (p_{f,\theta} \circ g_\theta) d\eta}_II \quad (54)$$

$$+ \underbrace{\int \|\nabla_x f \circ g_\theta \nabla_\theta g_\theta\| |p_{f,\theta} \circ g_\theta - p_{f,\theta'} \circ g_{\theta'}| d\eta}_III \quad (55)$$

The first term can be upper-bounded using  $L$ -smoothness of  $f$  and the fact that  $g_\theta$  is Lipschitz in  $\theta$ :

$$I \leq L\|\theta - \theta'\| \int |a|^2 (p_{f,\theta} \circ g_\theta) d\eta \quad (56)$$

$$\leq LC\|\theta - \theta'\| \quad (57)$$

Similarly, using that  $\nabla_\theta g_\theta$  is Lipschitz, it follows:

$$II \leq L\|\theta - \theta'\| \int |b| (p_{f,\theta} \circ g_\theta) d\eta \quad (58)$$

$$\leq LC\|\theta - \theta'\| \quad (59)$$

Finally, for the last term  $III$ , we first consider a path  $\theta_t = t\theta + (1-t)\theta'$  for  $t \in [0, 1]$  and introduce the function  $s(t) := p_{f,\theta_t} \circ g_{\theta_t}$ . We will now control the difference  $p_{f,\theta} \circ g_\theta - p_{f,\theta'} \circ g_{\theta'}$  also equal to  $s(1) - s(0)$ . Using the fact that  $s_t$  is absolutely continuous we have that  $s(1) - s(0) = \int_0^1 s'(t) dt$ . The derivative  $s'(t)$  is simply given by  $s'(t) = (\theta - \theta')^\top (M_t - \bar{M}_t) s(t)$  where  $M_t = (\nabla_x f \circ g_{\theta_t}) \nabla_\theta g_{\theta_t}$  and  $\bar{M}_t = \int M_t p_{f,\theta_t} \circ g_{\theta_t} d\eta$ . Hence,

$$s(1) - s(0) = (\theta - \theta')^\top \int_0^1 (M_t - \bar{M}_t) s(t) dt \quad (60)$$

We also know that  $M_t$  is upper-bounded by  $La$  which implies the following inequalities:

$$III \leq L^2 \|\theta - \theta'\| \int_0^1 |a|^2 s(t) d\eta \quad (61)$$

$$\leq 2L^2 C \|\theta - \theta'\| \quad (62)$$

This allows to conclude that  $\mathcal{L}_\theta(f)$  is  $L$ -smooth for any  $f \in \mathcal{E}$  and  $\theta \in \Theta$ .  $\square$

## B. Convergence rates of KALE

Here,  $\mathcal{H}$  is a Reproducing kernel Hilbert space of functions defined on a domain  $\mathcal{X} \subset \mathbb{R}^d$  and with kernel  $k$ . We consider  $\mathbb{P}$  and  $\mathbb{Q}$  two probability distributions on  $\mathcal{X}$  and  $\hat{\mathbb{P}}$  and  $\hat{\mathbb{Q}}$  their empirical versions given by:

$$\hat{\mathbb{P}} := \frac{1}{N} \sum_{n=1}^N \delta_{X_n}, \quad \hat{\mathbb{Q}} := \frac{1}{N} \sum_{n=1}^N \delta_{Y_n} \quad (63)$$

where  $(X_n)_{1 \leq n \leq N}$  and  $(Y_n)_{1 \leq n \leq N}$  are i.i.d. samples from  $\mathbb{P}$  and  $\mathbb{Q}$ . We also define the population and empirical objective functionals:

$$\mathcal{F}(h) := - \int h d\mathbb{P} - \int \exp(-h) d\mathbb{Q} + 1, \quad (64)$$

$$\hat{\mathcal{F}}(h) := - \int h d\hat{\mathbb{P}} - \int \exp(-h) d\hat{\mathbb{Q}} + 1. \quad (65)$$

We are interested in estimating  $\text{KL}(\mathbb{P} \parallel \mathbb{Q})$  that is obtained as a solution to the functional optimization problem:

$$\text{KL}(\mathbb{P} \parallel \mathbb{Q}) = \sup_{h \in \mathcal{H}} \mathcal{F}(h). \quad (66)$$

Here, we assumed that the negative log-density ratio  $h_0 := -\log(r_0)$  between  $\mathbb{P}$  and  $\mathbb{Q}$  exists and belongs to  $\mathcal{H}$ . This directly implies that the supremum of  $\mathcal{F}$  is achieved at  $h_0$  and  $\mathcal{F}(h_0) = \text{KL}(\mathbb{P} \parallel \mathbb{Q})$ . The proposed estimator is obtained by solving a regularized empirical problem:

$$\sup_{h \in \mathcal{H}} \hat{\mathcal{F}}(h) - \frac{\lambda}{2} \|h\|^2, \quad (67)$$

with a corresponding population version:

$$\sup_{h \in \mathcal{H}} \mathcal{F}(h) - \frac{\lambda}{2} \|h\|^2. \quad (68)$$

Finally, we introduce  $D(h, \delta)$  and  $\Gamma(h, \delta)$ :

$$D(h, \delta) = \int \delta \exp(-h) d\mathbb{Q} - \int \delta d\mathbb{P} \quad (69)$$

$$\Gamma(h, \delta) = - \int \int_0^1 (1-t) \delta^2 \exp(-(h + t\delta)) d\mathbb{Q}. \quad (70)$$

The empirical versions of  $D(h, \delta)$  and  $\Gamma(h, \delta)$  are denoted  $\hat{D}(h, \delta)$  and  $\hat{\Gamma}(h, \delta)$ . Later, we will show that  $D(h, \delta)$  and  $\hat{D}(h, \delta)$  are in fact the gradients of  $\mathcal{F}(h)$  and  $\hat{\mathcal{F}}(h)$  along the direction  $\delta$ .

We state now the working assumptions:

(A) The supremum of  $\mathcal{F}$  over  $\mathcal{H}$  is attained at  $h_0$ .

(B) The following quantities are finite for some positive  $\epsilon$ :

$$\int \sqrt{k(x, x)} d\mathbb{P}(x) \quad (71)$$

$$\int \sqrt{k(x, x)} \exp((\|h_0\| + \epsilon) \sqrt{k(x, x)}) d\mathbb{Q}(x) \quad (72)$$

$$\int k(x, x) \exp((\|h_0\| + \epsilon) \sqrt{k(x, x)}) d\mathbb{Q}(x) \quad (73)$$

(C) For any  $h \in \mathcal{H}$ , if  $D(h, \delta) = 0$  for all  $\delta$  then  $h = h_0$ .

We begin by the following lemma which provides an expression for  $D(h, \delta)$  and  $\widehat{D}(h, \delta)$  along with a probabilistic bound:

**Lemma 9.** *Under Assumptions (A) and (B), for any  $h \in \mathcal{H}$  such that  $\|h\| \leq \|h_0\| + \epsilon$ , there exists  $\mathcal{D}(h)$  in  $\mathcal{H}$  satisfying:*

$$D(h, \delta) = \langle \delta, \mathcal{D}(h) \rangle \quad (74)$$

And for any  $h \in \mathcal{H}$ , there exists  $\widehat{D}(h)$  satisfying:

$$\widehat{D}(h, \delta) = \langle \delta, \widehat{D}(h) \rangle \quad (75)$$

Moreover, for any  $0 < \eta < 1$  and any  $h \in \mathcal{H}$  such that  $\|h\| \leq \|h_0\| + \epsilon := M$ , it holds with probability greater than  $1 - \eta$  that:

$$\|\mathcal{D}(h) - \widehat{D}(h)\| \leq \frac{C(M, \eta)}{\sqrt{N}} \quad (76)$$

where  $C(M, \eta)$  depends only on  $M$  and  $\eta$ .

*Proof.* First, we show that  $\delta \mapsto D(h, \delta)$  is a bounded linear operator. Indeed, Assumption (B) ensures that  $k(x, \cdot)$  and  $k(x, \cdot) \exp(-h(x))$  are Bochner integrable w.r.t. to  $\mathbb{P}$  and  $\mathbb{Q}$  (Rutherford, 1978) hence  $D(h, \delta)$  is obtained as:

$$D(h, \delta) := \langle \delta, \mu_{\exp(-h)\mathbb{Q}} - \mu_{\mathbb{P}} \rangle \quad (77)$$

where  $\mu_{\exp(-h)\mathbb{Q}} = \int k(x, \cdot) \exp(-h(x)) d\mathbb{Q}$  and  $\mu_{\mathbb{P}} = \int k(x, \cdot) d\mathbb{P}$ . Defining  $\mathcal{D}(h)$  to be  $= \mu_{\exp(-h)\mathbb{Q}} - \mu_{\mathbb{P}}$  leads to the desired result.  $\widehat{D}(h)$  is simply obtained by taking the empirical version of  $\mathcal{D}(h)$ .

Finally, the probabilistic inequality is a simple consequence of Chebychev's inequality.  $\square$

The next lemma states that  $\mathcal{F}(h)$  and  $\widehat{\mathcal{F}}(h)$  are Frechet differentiable:

**Lemma 10.** *Under Assumptions (A) and (B),  $h \mapsto \mathcal{F}(h)$  is Frechet differentiable on the open ball of radius  $\|h_0\| + \epsilon$  while  $h \mapsto \widehat{\mathcal{F}}(h)$  is Frechet differentiable on  $\mathcal{H}$ . Their gradients are given by  $\mathcal{D}(h)$  and  $\widehat{D}(h)$  as defined in Lemma 9:*

$$\nabla \mathcal{F}(h) = \mathcal{D}(h), \quad \nabla \widehat{\mathcal{F}}(h) = \widehat{D}(h) \quad (78)$$

*Proof.* The empirical functional  $\widehat{\mathcal{F}}(h)$  is differentiable since it is a finite sum of differentiable functions and its gradient is simply given by  $\widehat{D}(h)$ . For the population functional, we use second order Taylor expansion of  $\exp$  with integral remainder which gives:

$$\mathcal{F}(h + \delta) = \mathcal{F}(h) - D(h, \delta) + \Gamma(h, \delta). \quad (79)$$

By Assumption (B) we know that  $\frac{\Gamma(h, \delta)}{\|\delta\|}$  converges to 0 as soon as  $\|\delta\| \rightarrow 0$ . This allows to directly conclude that  $\mathcal{F}$  is Frechet differentiable with differential given by  $\delta \mapsto D(h, \delta)$ . By Lemma 9, we conclude the existence of a gradient  $\nabla \mathcal{F}(h)$  which is in fact given by  $\nabla \mathcal{F}(h) = \mathcal{D}(h)$ .  $\square$

From now on, we will only use the notation  $\nabla \mathcal{F}(h)$  and  $\nabla \widehat{\mathcal{F}}(h)$  to refer to the gradients of  $\mathcal{F}(h)$  and  $\widehat{\mathcal{F}}(h)$ . The following lemma states that (67) and (68) have a unique global optimum and gives a first order optimality condition.

**Lemma 11.** *The problems (67) and (68) admit unique global solutions  $\hat{h}$  and  $h_\lambda$  in  $\mathcal{H}$ . Moreover, the following first order optimality conditions hold:*

$$\lambda \hat{h} = \nabla \widehat{\mathcal{F}}(\hat{h}), \quad \lambda h_\lambda = \nabla \mathcal{F}(h_\lambda). \quad (80)$$

*Proof.* For (67), existence and uniqueness of a minimizer  $\hat{h}$  is a simple consequence of continuity and strong concavity of the regularized objective. Now we show the existence result for (68). Let's introduce  $\mathcal{G}_\lambda(h) = -\mathcal{F}(h) + \frac{\lambda}{2} \|h\|^2$  for simplicity. Uniqueness is a simple consequence of strong convexity of  $\mathcal{G}_\lambda$ . For the existence, consider a sequence of elements  $f_k \in \mathcal{H}$  such that  $\mathcal{G}_\lambda(f_k) \rightarrow \inf_{h \in \mathcal{H}} \mathcal{G}_\lambda(h)$ . If  $h_0$  is not the global solution, then it must hold for  $k$  large enough that  $\mathcal{G}_\lambda(f_k) \leq \mathcal{G}_\lambda(h_0)$ . We also know that  $\mathcal{F}(f_k) \leq \mathcal{F}(h_0)$ , hence, it is easy to see that  $\|f_k\| \leq \|h_0\|$  for  $k$  large enough. This implies that  $f_k$  is a bounded sequence, therefore it admits a weakly convergent sub-sequence by weak compactness. Without loss of generality we assume that  $f_k$  weakly converges to some element  $h_\lambda \in \mathcal{H}$  and that  $\|f_k\| \leq \|h_0\|$ . Hence,  $\|h_\lambda\| \leq \liminf_k \|f_k\| \leq \|h_0\|$ . Recall now that by definition of weak convergence, we have  $f_k(x) \rightarrow_k h_\lambda(x)$  for all  $x \in \mathcal{X}$ . By Assumption (B), we can apply the dominated convergence theorem to ensure that  $\mathcal{F}(f_k) \rightarrow \mathcal{F}(h_\lambda)$ . Taking the limit of  $\mathcal{G}_\lambda f_k$ , the following inequality holds:

$$\sup_{h \in \mathcal{H}} \mathcal{G}_\lambda(h) = \limsup_k \mathcal{G}_\lambda(f_k) \leq \mathcal{G}_\lambda(h_\lambda). \quad (81)$$

Finally, by Lemma 10 we know that  $\mathcal{F}$  is Frechet differentiable, hence we can use (Ekeland & Témam, 1999) (Proposition 2.1) to conclude that  $\nabla \mathcal{F}(h_\lambda) = \lambda h_\lambda$ . We use exactly the same arguments for (67).  $\square$

Next, we show that  $h_\lambda$  converges towards  $h_0$  in  $\mathcal{H}$ :

**Lemma 12.** *Under Assumptions (A) to (C) it holds that:*

$$\mathcal{A}(\lambda) := \|h_\lambda - h_0\| \rightarrow 0. \quad (82)$$

*Proof.* We will first prove that  $h_\lambda$  converges weakly towards  $h_0$  and then conclude that it must also converge strongly. We start by noticing the following inequalities:

$$0 \geq \mathcal{F}(h_\lambda) - \mathcal{F}(h_0) \geq \frac{\lambda}{2} (\|h_\lambda\|^2 - \|h_0\|^2). \quad (83)$$

These are simple consequences of the definitions of  $h_\lambda$  and  $h_0$  as optimal solutions to (66) and (67). This implies that  $\|h_\lambda\|$  is always bounded by  $\|h_0\|$ . Consider now an arbitrary sequence  $(\lambda_m)_{m \geq 0}$  converging to 0. Since  $\|h_{\lambda_m}\|$  is bounded by  $\|h_0\|$ , it follows by weak-compactness of balls in  $\mathcal{H}$  that  $h_{\lambda_m}$  admits a weakly convergent sub-sequence. Without loss of generality we can assume that  $h_{\lambda_m}$  is itself weakly converging towards an element  $h^*$ . We will show now that  $h^*$  must be equal to  $h_0$ . Indeed, by optimality of  $h_{\lambda_m}$ , the following equation must hold:

$$\lambda_m h_{\lambda_m} = \nabla \mathcal{F}(h_m). \quad (84)$$

This implies that  $\nabla \mathcal{F}(h_m)$  converges weakly to 0. On the other hand, by Assumption (B), we can conclude that  $\nabla \mathcal{F}(h_m)$  must also converge weakly towards  $\nabla \mathcal{F}(h^*)$ , hence  $\nabla \mathcal{F}(h^*) = 0$ . Finally by Assumption (C) we know that  $h_0$  is the unique solution to the equation  $\nabla \mathcal{F}(h) = 0$ , hence  $h^* = h_0$ . We have shown so far that any subsequence of  $h_{\lambda_m}$  that converges weakly, must converge weakly towards  $h_0$ . This allows to conclude that  $h_{\lambda_m}$  actually converges weakly towards  $h_0$ . Moreover, we also have by definition of weak convergence that:

$$\|h_0\| \leq \liminf_{m \rightarrow \infty} \|h_{\lambda_m}\|. \quad (85)$$

Recalling now that  $\|h_{\lambda_m}\| \leq \|h_0\|$  it follows that  $\|h_{\lambda_m}\|$  converges towards  $\|h_0\|$ . Hence, we have the following two properties:

- $h_{\lambda_m}$  converges weakly towards  $h_0$ .
- $\|h_{\lambda_m}\|$  converges towards  $\|h_0\|$ .

This allows to directly conclude that  $\|h_{\lambda_m} - h_0\|$  converges to 0.  $\square$

**Proposition 13.** *We have that:*

$$\|\hat{h} - h_\lambda\| \leq \frac{1}{\lambda} \|\nabla \hat{\mathcal{F}}(h_\lambda) - \nabla \mathcal{F}(h_\lambda)\| \quad (86)$$

*Proof.* By definition of  $\hat{h}$  and  $h_\lambda$  the following optimality conditions hold:

$$\lambda \hat{h} = \nabla \hat{\mathcal{F}}(\hat{h}), \quad \lambda h_\lambda = \nabla \mathcal{F}(h_\lambda). \quad (87)$$

We can then simply write:

$$\lambda(\hat{h} - h_\lambda) - (\nabla \hat{\mathcal{F}}(\hat{h}) - \nabla \hat{\mathcal{F}}(h_\lambda)) = \nabla \hat{\mathcal{F}}(h_\lambda) - \nabla \mathcal{F}(h_\lambda) \quad (88)$$

Now introducing  $\delta := \hat{h} - h_\lambda$  and  $E := \nabla \hat{\mathcal{F}}(\hat{h}) - \nabla \hat{\mathcal{F}}(h_\lambda)$  for simplicity and taking the squared norm of the above equation, it follows:

$$\lambda^2 \|\delta\|^2 + \|E\|^2 - 2\lambda \langle \delta, E \rangle = \|\nabla \hat{\mathcal{F}}(h_\lambda) - \nabla \mathcal{F}(h_\lambda)\|^2 \quad (89)$$

By concavity of  $\hat{\mathcal{F}}$  on  $\mathcal{H}$  we know that  $-\langle \hat{h} - h_\lambda, E \rangle \geq 0$ . Therefore:

$$\lambda^2 \|\hat{h} - h_\lambda\|^2 \leq \|\nabla \hat{\mathcal{F}}(h_\lambda) - \nabla \mathcal{F}(h_\lambda)\|^2. \quad (90)$$

$\square$

We can now provide a proof for Theorem 6.

*Proof of Theorem 6.* Notice the following inequalities:

$$\frac{\lambda}{2} (\|\hat{h}\|^2 - \|h_0\|^2) \leq \hat{\mathcal{F}}(\hat{h}) - \hat{\mathcal{F}}(h_0) \leq \langle \nabla \hat{\mathcal{F}}(h_0), \hat{h} - h_0 \rangle. \quad (91)$$

The first inequality is by definition of  $\hat{h}$  while the second is obtained by concavity of  $\hat{\mathcal{F}}$ . For simplicity we write  $\mathcal{B} = \|\hat{h} - h_0\|$  and  $\mathcal{C} = \|\nabla \hat{\mathcal{F}}(h_0) - \mathcal{L}(h_0)\|$ . Using Cauchy-Schwarz and triangular inequalities, it is easy to see that:

$$-\frac{\lambda}{2} (\mathcal{B}^2 + 2\mathcal{B}\|h_0\|) \leq \hat{\mathcal{F}}(\hat{h}) - \hat{\mathcal{F}}(h_0) \leq \mathcal{C}\mathcal{B} \quad (92)$$

Moreover, by triangular inequality it holds that:

$$\mathcal{B} \leq \|h_\lambda - h_0\| + \|\hat{h} - h_\lambda\|$$

Lemma 12 ensures that  $\mathcal{A}(\lambda) = \|h_\lambda - h_0\|$  converges to 0 as  $\lambda \rightarrow 0$ . Furthermore, by Proposition 13 we have  $\|\hat{h} - h_\lambda\| \leq \frac{1}{\lambda} \mathcal{D}$  where  $\mathcal{D}(\lambda) = \|\nabla \hat{\mathcal{F}}(h_\lambda) - \nabla \mathcal{L}(h_\lambda)\|$ . Now choosing  $\lambda = \frac{1}{\sqrt{N}}$  and applying Chebychev inequality in Lemma 9, it follows that for any  $1 > \eta > 0$  we have with probability greater than  $1 - 2\eta$  that both:

$$\mathcal{D}(\lambda) \leq \frac{C(\|h_0\|, \eta)}{\sqrt{N}}, \quad \mathcal{C} \leq \frac{C(\|h_0\|, \eta)}{\sqrt{N}} \quad (93)$$

Where  $C(\|h_0\|, \eta)$  is defined in Lemma 9. This allows to conclude that for any  $\eta > 0$ , it holds with probability at least  $1 - 2\eta$  that  $|\hat{\mathcal{F}}(\hat{h}) - \hat{\mathcal{F}}(h_0)| \leq \frac{M'(\eta, h_0)}{\sqrt{N}}$  where  $M'(\eta, h_0)$  depends only on  $\eta$  and  $h_0$ .  $\square$

## C. Adversarial training for Energy models

**Algorithm 3** KALE-GAN

---

```

1: Input  $N, \lambda, n_{\mathcal{G}}, n_{\mathcal{E}}, \gamma_{\mathcal{G}}, \gamma_{\mathcal{E}}, \mathbb{P}$ 
2: Output  $\mathbb{Q}_{g_{n_{\mathcal{G}}}} \exp(-h_{n_{\mathcal{G}}})$ 
3: Initialize  $\theta_0$  and set  $g_0 \leftarrow g_{\theta_0}$ 
4: Initialize  $(\psi_0, c_0)$  and set  $h_0 \leftarrow f_{\psi_0} + c_0$ .
5: for  $k = 0, \dots, n_{\mathcal{G}} - 1$  do
6:    $h_k \leftarrow \text{KALE-energy}(N, \lambda, n_{\mathcal{E}}, \gamma_{\mathcal{E}}, h_k, \mathbb{P}, \mathbb{Q}_{g_k})$ 
7:    $X_i \sim \mathbb{P}$  and  $Y_i \sim \mathbb{Q}$  for  $1 \leq i \leq N$ 
8:   Compute  $\widehat{\text{KALE}}(\mathbb{P}, \mathbb{Q}_{g_k}) = \widehat{\mathcal{F}}(h_k)$ 
9:   Compute gradient of  $\widehat{\text{KALE}}(\mathbb{P}, \mathbb{Q}_{g_k})$  w.r.t.  $(\theta)$ :
     $\Delta\theta \leftarrow \nabla_{\theta} \widehat{\text{KALE}}(\mathbb{P}, \mathbb{Q}_{g_k})$ 
10:  Update base:  $\theta_{k+1} \leftarrow \theta_k - \gamma_{\mathcal{G}} \Delta\theta$ 
     $g_{k+1} \leftarrow g_{\theta_{k+1}}$ 
11: end for
12:  $h_{n_{\mathcal{G}}} \leftarrow \text{KALE-energy}(N, \lambda, n_{\mathcal{E}}, \gamma_{\mathcal{E}}, h_{n_{\mathcal{G}}-1}, \mathbb{P}, \mathbb{Q}_{g_{n_{\mathcal{G}}}})$ 

```

---

## D. Experimental details

### D.1. UCI

We use an EBM where the energy function is parameterized by a network with 3 hidden layers with (1000, 2000, 1000) being the number of unit for each layer. For the base distribution, we use a **MADE** network (Germain et al., 2015) with 3 autoregressive hidden layers, each one of them having  $10^3$  units. We train the MADE model using SGD with mini-batches of size 100 and an initial learning rate of  $10^{-5}$  for 1000 epoch and keep the model that reaches the highest value of the likelihood on the validation set. To avoid overfitting, a small amount of  $L_2$ -regularization on the weights was used for MADE with a penalty strength of  $10^{-4}$  to  $10^{-6}$ . Once the base model was optimized, we then learn the energy models by maximizing the objective (6). For the regularization  $I(f + c)$ , we use a combination of  $L_2$  norm and a variant of the gradient penalty (Gulrajani et al., 2017):

$$I(f_{\psi} + c)^2 = \frac{1}{d_{\psi}} \|\psi\|^2 + \mathbb{E} \left[ \|\nabla_x f_{\psi}(\widetilde{X})\|^2 \right] \quad (94)$$

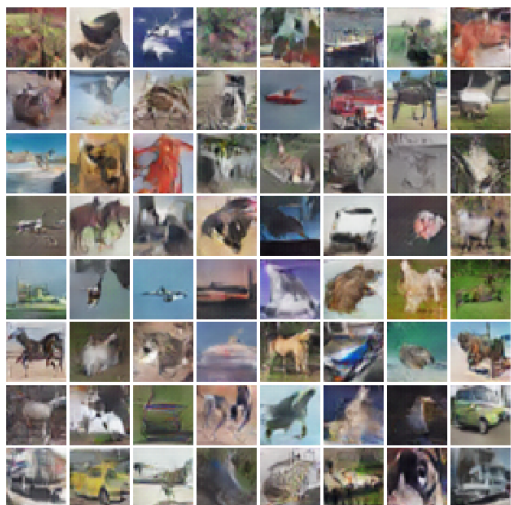
where  $d_{\psi}$  is the dimension of the parameter  $\psi$  and the expectation in the second term is taken over samples  $\widetilde{X}$  of the form  $\widetilde{X} = tX + (1 - t)Y$  with  $X \sim \mathbb{P}$ ,  $Y \sim \mathbb{Q}$  and  $t$  is a uniform on  $[0, 1]$ . We use the value  $\lambda = \frac{0.1}{\sqrt{N}}$  for the strength of the penalty where  $N$  is the size of the training set. The model is then trained for  $10^3$  epochs with an initial learning rate of  $10^{-4}$  and a batch-size of 100. The learning rate is decreased by 0.1 at epochs 50, 500 and 750. The results are then reported on the test set for the model that achieves the highest likelihood on the validation set.

### D.2. CIFAR10

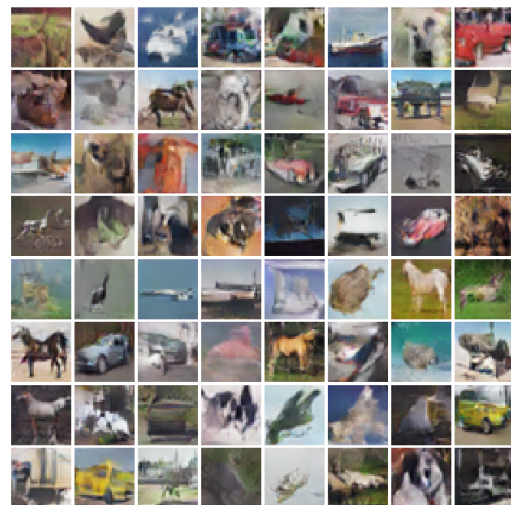
We train the energy models for 100 epochs with a batch size of 128. We varied the learning rate across models from

$10^{-5}$  to  $10^{-4}$ . In some models, we also added a gradient penalty as in (94), and in other models we included spectral normalization as in (Miyato et al., 2018).

We used Langevin Monte Carlo (Algorithm 3) for sampling posteriors, with a step-size of  $\gamma = 0.01$  and a friction coefficient  $\kappa = 0.04$ . Good-quality samples (as shown with lower FID scores) are generally present at about  $T = 80$  steps. In this work, we did not explore the large space of possible  $\gamma$  and  $\kappa$  hyperparameter settings; the ones given perform reasonably well and one could imagine a separate step of optimizing over the hyperparameters.



(a) Samples from the generator only.



(b) Samples from the energy model (DCGAN).